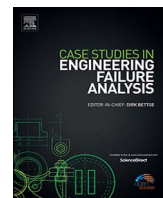




Contents lists available at ScienceDirect

Case Studies in Engineering Failure Analysis

journal homepage: www.elsevier.com/locate/csefa



Root cause failure analysis of a tracked vehicle balance arm



Ayaz M. Khan^{a,*}, Khalid Mahmood^b, Syed Waheed ul Haq^c, Rizwan Saeed Choudhry^d, Shahbaz Mahmood Khan^e

^a HITEC University, Taxila 47080, Pakistan

^b Department of Mechanical Engineering, CE & ME, National University of Sciences and Technology (NUST), Pakistan

^c Heavy Industries Taxila, Taxila Cantt, Pakistan

^d Department of Mechanical Engineering and the Built Environment, University of Derby, Derby, UK

^e Mechanical Engineering Department, Ghulam Ishaq Khan Institute of Engineering Sciences and Technology, Topi, Pakistan

ARTICLE INFO

Keywords:

Tracked vehicle
Balance arm
Failure analysis
Non-destructive testing
Fractography

ABSTRACT

This paper relates to an upgraded Industrial tracked vehicle which was found with a failed Balance arm during disassembly. The failure analysis of an actual Balance Arms surface was carried out using Fractography and Non Destructive testing techniques to dig out the root cause. The analysis revealed microscopic signatures categorically pointing towards post failure surface mechanical damage. The factor causing to promote failure was improper manufacturing i.e. casting which was further attributed to MnS inclusions.

1. Introduction

Suspension system plays a vital role in stability of a Tracked vehicle especially under dynamic loading. Suspension is a resilient damping unit to connect the hull of the tracked vehicle to the road wheels. It is used to lessen the shock of ground against the hull transmitted through the tracks and road wheels during the vehicles running's and decay the vehicle vibration and ensuring smooth running of the vehicle. To fulfil these requirements, four major parts i.e. Balance arms, torsion bars, shock absorbers, upper and lower bump stops are present. Balance arm is among the critical parts of a tracked vehicle which is subjected to bending, compression as well as torsional loads and on which weight of the whole vehicle is supported [1–3]. The Balance arm is assembled to road wheel on one side while with torsion bar on the other (See Fig. 1). As the tracked vehicle is generally subjected to severe loading conditions, thus, it is of high likelihood that its critical assemblies may fail or develop fatigue cracks. Loading conditions are, however, not the sole reason for early crack development. Systems are known to undergo mechanical failure due to defects in manufacturing, errors in design, discontinuities in casting, improper heat treatments as well [4]. If failure eventually results in fracture, fractography is usually carried out to know the root cause of failure by interpreting the fractographic features [5]. The goal of fractography is to locate the fracture origin based on the characteristics marks on the fractured sample such as beachmarks, chevrons and riverlines. These indicate direction of crack growth while fracture propagates. The researchers Gys van Zyl, Zhiwei et al, L.B Godefroid, Pantazopoulos [6–8] have worked on finding out the root cause of failure based on standard failure analysis procedure. The usual procedure followed in these papers was to characterize the material initially followed by analyzing the failed surface using non-destructive testing (NDT) and fractography. The root cause was then identified in the light of outcome of these analyses.

* Corresponding author.

E-mail address: engg_ayaz@hotmail.com (A.M. Khan).

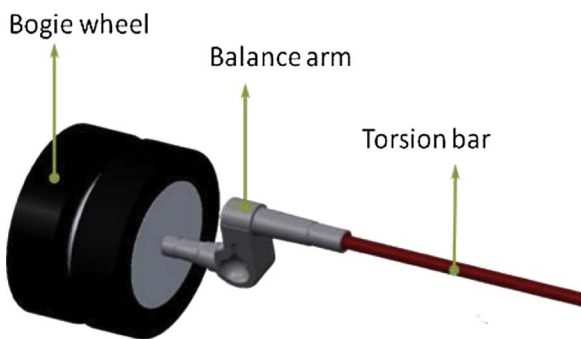


Fig. 1. Balance arm assembly (3D Model).

2. Background

The tracked vehicle discussed in this study has been previously upgraded by adding mass to strengthen the hull. This study is focused towards ascertaining the effect of added weight on the tracked vehicle Balance arms and find out the failure root cause. The complete sets of 10 Arms were inspected of which one was fractured and 6 were found with cracks. It is important to note that, the rebuild cycles of the tracked vehicle discussed in the present study are scheduled for every 9000 km track running, but the Arms of the upgraded vehicles (with body weight enhancements) were found either fractured or had produced cracks after only 5320 km running. The study was initiated in an event to carry out failure analysis for identifying the root cause. Although numerous failure case analysis studies can be found in literature for commercial vehicles [6], the same is not available for tracked vehicle. In fact to the best of authors knowledge there is no such study reported in International Journals of repute.

The Balance arm is initially characterized by investigating its chemical and mechanical properties. Moreover, Arm with fracture is investigated with visual and microscopic examinations. Furthermore, the Balance arms with cracks are examined using NDT. The results are then post processed to determine the crack displacement mode. All this methodology is presented in the subsequent sections.

3. Materials and methods

3.1. Chemical analysis

The Balance arm was characterized based on experimentation to obtain its chemical analysis using 60 channel spectrometer. The results of the chemical analysis are presented in Table 1.

3.2. Tensile testing

The sample for tensile testing was prepared in accordance to ASTM A370 standard [9]. Testing was then carried out on universal hydraulic testing machine. The Balance arm properties were best matched to being AISI 4340 steel based on both chemical and mechanical testing. The Balance arm mechanical properties are presented in Table 2.

3.3. Cross-sectional hardness profile

The complete hardness profile along the radial and longitudinal direction of the failed balance arm was investigated. The focus was to locate strain hardening (if any), however the profile was normal along both the directions. The results are depicted in Table 3.

3.4. Non-destructive testing

The procedure for Non-destructive testing was adopted from article 1, article 2 and article 6 of ASME Section V [10] for general guidelines, liquid penetrant techniques respectively. For liquid penetrant testing, the surface temperature was 22 °C.

Table 1

Results of chemical analysis of balance arm material.

C(%)	Mn(%)	Cr(%)	Ni(%)	Mo(%)	S(%)
0.5	0.75	0.6	0.8	0.15	0.05

Table 2
Mechanical properties of balance arm material.

Property	Value	Unit
Elastic Modulus	210	GPa
Tensile Strength	939	MPa
Yield Strength	715	MPa
Poisson's ratio	0.29	–
Reduction in area (%)	58	–
Elongation (%)	11	–
Hardness	270	HB

Table 3
Brinell hardness along radial and longitudinal direction.

Radial (HB)	Longitudinal (HB)
278	276
279	276
289	281
274	274
286	266
269	270
286	253
277	266
288	278
273	254
273	276
283	269
287	244
273	234
270	242

3.5. Microscopy

Microscopy was carried out using an analytical scanning electron microscope (JEOL, JSM6490A, Japan).

4. Results and discussion

4.1. Visual examination

The single fractured balance arm during tracked vehicles disassembly was visually examined to know the probable cause of failure/damage. The fracture surface shown in Fig. 2 was fairly flat with multiple crack initiation points. The cracks initiated from the spline teeth area near the internal diameter. Moreover, the final fast fracture has the typical appearance of brittle fracture. This evidently depicts no or little plastic deformation [11]. Also the Balance arms in general were found with corrosion.

4.2. Fractography

To explore the actual root cause of failure, the same naturally in-service broken balance arm found during disassembly of the tracked vehicle was analyzed at high magnifications under optical and scanning electron microscope. Firstly, the unpolished fracture surface was studied under SEM for failure signatures. The micrographs were obtained at different magnifications. A single

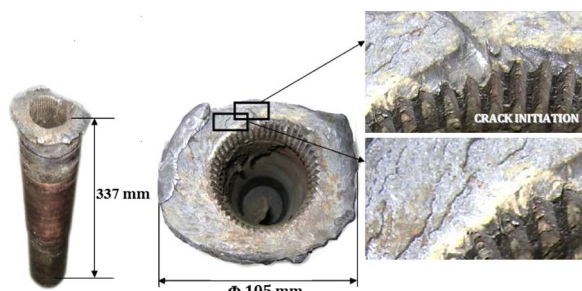


Fig. 2. Fractured balance arm.

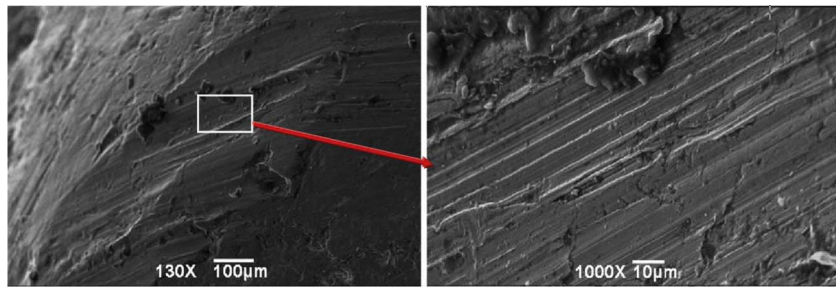


Fig. 3. (a) and (b) Post Failure Damage of the fracture surface.

Micrograph with its magnified counterpart is shown in Fig. 3a and b. The presented micrograph depicts post failure surface mechanical damage.

Subsequent to the observation of unpolished balance arm fractured surface, the polishing of samples was carried out for optical microscopy and SEM. Optical micrographs were observed at location A–D for the same fractured balance arm surface shown in Fig. 2. (See Table 4 for locations). It is pertinent to mention here that a fine grain microstructure with higher hardness value was observed on the sample. This is in agreement with the famous Hall-Petch relationship [16] which is as under:

$$\sigma_y = \sigma_o + k_y d^{-1/2}$$

Where d is the average grain diameter, σ_o and k_y and are constants for a particular material.

The Optical and SEM micrographs of polished cross-section are shown in Figs. 4 and 5 respectively. These micrographs reveal porosity close to internal bore, midway of the cross-section, close to the internal diameter and near external diameter. These locations are highly prone to develop cracks as fatigue cracks initiate on localized shear plane at or near porosity, inclusions, or discontinuities [12]. It is worth noting that the optical Micrograph presented in Fig. 4d reveal large sized pores of the order of about 100 μm which supports the fact that the cracks have initiated near internal diameter adjacent to bore having spline teeth. Both optical micrographs, SEM micrographs are seen to exhibit substantial porosity in the structure from sub-micron to as large as more than 100 μm . These discontinuities in metallic mass are due to non-metallic inclusions, which cause to reduce the strength, resistance to fatigue, etc. The two dominant inclusions in steel are MnS and Al₂O₃ [13]. During polishing for metallography this type of inclusions are leached out leaving behind pore-type appearance. The inclusions in Balance arm are attributed towards MnS inclusions as unexpectedly high sulphur content was observed during chemical analysis. MnS inclusions are categorized under non metallic inclusions which are detrimental to steels mechanical properties. Presence of MnS impurities leads to an improvement in machinability, however they facilitate crack propagation by acting as void nucleation sites. This indicates manufacturing fault during fabrication i.e. casting [13,14].

4.3. Liquid penetrant testing and crack displacement mode

A total of 10 Balance arms were inspected out of which one was found fractured during disassembly (as described earlier). The balance arms assembled in the tracked vehicle with their locations can be visualized in Fig. 6. The remaining 9 balance arms were to be inspected. The Machined portion of these balance arms was the area of interest. The balance Arms surface was prepared by cleaning the area to be examined and area in vicinity to make it free of any dirt, grease, etc. The surface was then dried using a dry lint free cloth before application of penetrant. A solvent removable penetrant type was applied and after a dwell time of 15 min, excess penetrant was removed from the surface. The surface was subsequently allowed to dry by natural evaporation. A Non-Aqueous Wet developer was then sprayed directly onto the surface. A dwell time of 10 min was allowed before starting for Inspection. The balance arms were inspected under a torch light for any surface flaws. 6 out of 9 balance arms were found with cracks. The crack lengths were directly measured for evaluation [10] by tracing the path of flaw formed due to the penetrant and developer application. The cracks were formed at multiple locations on each balance arm and considering the different lengths, a crack length range was established. The summary of these balance arms along with crack lengths and part numbers are presented in Table 5. The maximum observed crack size was 45 mm in balance arm with part number 7127.

The remaining 3 Arms were found free of cracks. The observed cracks were circumferential in nature and surprisingly all the cracks were seen at the hull side on the lower curvature of the balance arm surface (Fig. 7). The inspected 10 torsion bars, sprocket

Table 4
Details of optical micrographs

Location	Detail
A	Optical image close to internal bore having spline teeth ($\times 500$)
B	Optical image at midway of cross-section ($\times 500$)
C	Optical image close to outer diameter ($\times 200$)
D	Optical image near internal diameter adjacent to bore having spline teeth ($\times 200$)

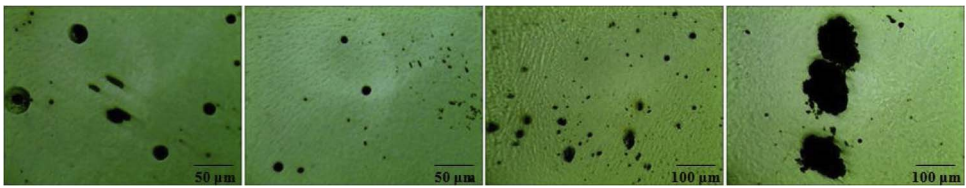


Fig. 4. Optical micrographs at (a) location A, $\times 500$; (b) location B, $\times 500$; (c) location C, $\times 200$; (d) location D.

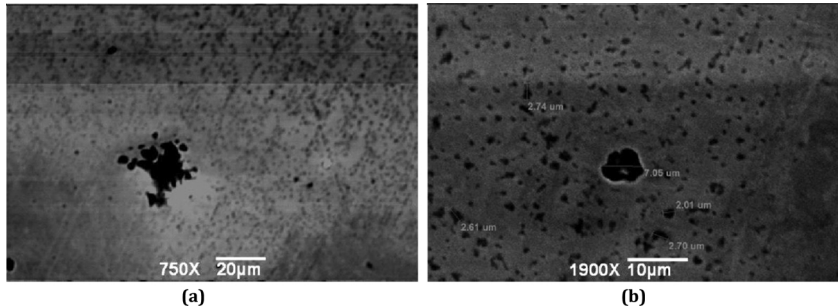


Fig. 5. (a) and (b) SEM micrographs showing porosity at 750 \times and 1900 \times magnification.

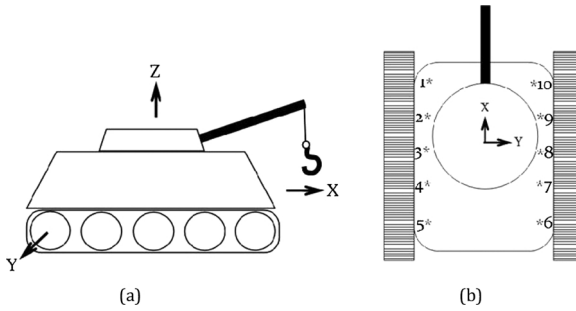


Fig. 6. (a) Coordinate system; (b) balance arm assembly locations.

Table 5
Test Parts for non-destructive testing.

S. No.	Location	Crack length (mm)	Defect	Part No
1	On Hull side	5–30	Cracking	2748
2	On Hull side	2–25	Cracking	952
3	On Hull side	5–45	Cracking	7127
4	On Hull side	6–40	Cracking	6723
5	On Hull side	2–20	Cracking	61110
6	On Hull side	6–35	Cracking	90687

wheel and related components/assemblies were found free of cracks. The maximum obtained crack length was utilized for finding the loading condition & state of stress at the crack tip. To ensure that state of stress at the tip of the crack is elastic plain strain over most of the length of the crack tip, following condition should be satisfied [15]:

$$a, t \geq 2.5 \left(\frac{K_{IC}}{\sigma_Y} \right)^2$$

Where K_{IC} is the Critical Stress Intensity factor, σ_Y is the yield strength of the material, a and t are crack length and thickness respectively. If the dimensions of the member are such that the state of stress over most of the length of the crack tip is plane strain, the crack will propagate with minimum plastic deformation occurring at the crack tip. The material in such members is considered to be loaded in the brittle state [14,15]. In order to have a fair idea about the loading condition; state of stress at the tip of crack, above said equation was used. The required parameters comprising arm thickness of balance arm and maximum obtained crack length are 0.025 m and 0.045 m respectively. The critical stress intensity factor for AISI 4340 (i.e. $K_{IC} = 59 \text{ MPa}\sqrt{\text{m}}$) is selected based on the material characterization [11]. Evaluating above said equation yields 0.045, 0.025 0.0170 which satisfies the relation and proves the



Fig. 7. Liquid penetrant tests revealing cracks in various balance arms of the upgraded Tracked vehicle.

fact that state of stress at the crack tip is elastic plane strain. Based on the above findings, the loading condition & state of stress is categorized as elastic plane strain condition and the material is loaded in brittle state.

5. Conclusions

This study was performed to analyze balance arms being fractured or develop cracks before their scheduled rebuild cycles. To do the same; the cause of failure was determined using visual inspection, microscopy and Non-destructive testing. The conclusions are presented below:

- The Balance Arms were seen with corrosion. There must be anti corrosion agents used to minimize corrosion due to environmental conditions.
- Visual examination of Balance arm revealed failure that was observed to be flat having brittle fracture characteristics and multiple crack initiation points. During SEM, post fracture mechanical damage was observed in the micrographs. In addition, substantial porosity of was observed during SEM and optical Microscopy of polished surface. The large size voids observed during SEM and Optical microscopy were attributed to MnS inclusions. This finding was further related to manufacturing fault. To avoid early crack development, the manufacturing procedure needs to be changed.
- During Liquid penetration technique, 6 arms were observed with significant cracks in the portion fitted inside the hull body of the tracked vehicle. The cracks were along the circumference on the lower semicircular arc of the Balance arm. All the cracks were observed towards the hull side. The third left arm was found fractured. The cracks initiated and propagated along the x-axis. During NDT results post-processing it was found out that the state of stress at the tip of the crack is elastic plain strain, Balance arm is loaded in brittle state. The Balance arm design needs to be modified to reinforce the area where cracks have been identified to initiate.

References

- [1] Dhir Anil, Sankar Seshadri. Assessment of tracked vehicle suspension system using a validated computer simulation model. *J Terramech* 1995;32(3):127–49.
- [2] Hohl GH. Torsion-bar spring and damping systems of tracked vehicles. *J Terramech* 1985;22(4):195–203.
- [3] Yu Xiaoming, Chang Kuang-Hua, Choi Kyung K. Probabilistic structural durability prediction. *AIAA J* 1998;36(4):628–37.
- [4] Popov Egor Paul. *Engineering Mechanics of Solids*. 2nd ed. Upper Saddler River, NJ: Prentice Hall; 1999. (Print).
- [5] Mills Kathleen. *Fractography Vol. 12*. Materials Park, OH: ASM International; 2009. (Print).
- [6] Yu Zhiwei, Xiaolei Xu. Failure analysis of a diesel engine crankshaft. *Eng Fail Anal* 2005;12(3):487–95.
- [7] Godefroid Leonardo Barbosa, et al. Fatigue failure of a welded automotive component. *Procedia Mater Sci* 2014;3:1902–7.
- [8] Pantazopoulos George, et al. Analysis of abnormal fatigue failure of forklift forks. *Case Stud Eng Fail Anal* 2014;2(2):9–14.
- [9] ASTM A370-17. *Standard Test Methods and Definitions for Mechanical Testing of Steel Products*. West Conshohocken, PA: ASTM International; 2017 www.astm.org.
- [10] Nondestructive Examination: ASME Boiler and Pressure Vessel Code: Section V. New York: American Society of Mechanical Engineers; 1977. (Print).
- [11] Meyers Marc A, Krishan Kumar Chawla. *Mechanical behavior of materials Vol. 2*. Cambridge: Cambridge University Press; 2009.
- [12] Lee Yung-Li. *Fatigue testing and analysis: theory and practice vol. 13*. Butterworth-Heinemann; 2005.
- [13] Sohaciuc M, et al. Influence of MnS inclusions in steel parts on fatigue resistance. *Dig (DJNB)* 2013;8(1):367–76.
- [14] Boresi Arthur Peter, Schmidt Richard Joseph, Sidebottom Omar M. *Advanced mechanics of materials Vol. 6*. New York: Wiley; 1993.
- [15] Totten George. *Fatigue crack propagation*. *Adv Mater Processes* 2008;166(5):39.
- [16] Callister Jr. William D. *Materials Science and Engineering An Introduction*. 7th edition John Wiley & Sons Inc; 2007. p. 189.